Mathematical Biosciences and Engineering

MBE, 16(5): 4607–4621
DOI: 10.3934/mbe.2019231
Received: 28 February 2019
Accepted: 19 April 2019
Published: 23 May 2019

http://www.aimspress.com/journal/MBE

Research article

MicroRNA-527 inhibits TGF-β/SMAD induced epithelial-mesenchymal transition via downregulating SULF2 expression in non-small-cell lung cancer

Wei Huo, Xiao-Min Zhu, Xin-Yan Pan, Min Du, Zhuo Sun and Zhi-Min Li *

Department of Medical Oncology, Dalian Municipal Central Hospital Affiliated of Dalian Medical University, Dalian 116033, China.

*** Correspondence:** Email: dlzlklzm0314@163.com; Tel: +86-0411-84412001.

Abstract: Objective: To explore the potential mechanism which miR-527 targeting the heparan sulfate 6-O-endosulfatase (SULF2) regulates TGF-β/SMAD signaling pathway induced epithelial-mesenchymal transition (EMT) in non-small-cell lung cancer (NSCLC). Methods: 38 pairs of lung tumor biopsies and corresponding paracancerous biopsies were obtained from NSCLC patients with surgical resection, normal human bronchial epithelial BEAS-2B cells and five NSCLS cell lines were applied for our study. miR-527 and SULF2 expression were determined by qRT-PCR and immunohistochemistry. MiR-527 and SULF2 biological link were predicted by Targetscan.org and tested by dual luciferase. Cells proliferation and apoptosis were respectively detected by EDU staining and flow cytometry. Cells migration was examined by transwell and scratch-wound assay. Expression of proteins related to EMT and TGF-β/SMAD signaling pathway, such as E-cadherin, N-cadherin, p-Samd3 and p-Smad2, was detected by western blot. Results: miR-527 expression was decreased in lung tumor tissues and NSCLS cell lines, conversely, SULF2 expression was significantly increased. In addition, we found that miR-527 targeted 3'-untranslated regions (3'-UTR) of SULF2 and mediated its expression. Overexpression of miR-527 evidently suppressed NSCLC proliferation, invasion and EMT via TGF-β/SMAD signaling pathway. Moreover, the silence of SULF2 exhibited a similar effect. Conclusion: miR-527 targeting SULF2 down-regulated SULF2 expression, concurrently, suppressed NSCLC epithelial-mesenchymal transition and invasion via inhibiting TGF-β/SMAD signaling pathway.

Keywords: miR-527; SULF2; TGF-β/SMAD signaling pathway; NSCLC; EMT

1. Introduction

Lung cancer remains the maximum cause of cancer-related death around the world, and non-small cell lung cancer (NSCLC) approximately accounts for 84% of all lung cancer cases histopathologically classified [1,2]. Regrettably, the majority of patients with NSCLC were diagnosed at the terminal stage. However, the effectiveness of current therapies aiming to treatment and prognosis of NSCLS is very limited, because the potential biomarker for molecular targeted therapy and individualized therapy is not available. Consequently, it is an imperious demand to optimize molecular genetic diagnosis and prognosis for molecular targeted therapy and clinical decision-making [3].

Previous studies showed that cancer cells underwent phenotypic changes from epithelia towards mesenchyme transition, and lung cancer cells generally present mesenchymal phenotype [4,5]. The most apparent hallmark of EMT is that different genes respectively regulate epithelial and mesenchymal phenotype, and increased biomarker of mesenchyme accompanied with decreased biomarker of epithelia is highly relevant to EMT. Numerous studies have confirmed that TGF-β1 is the most important factor in inducing EMT [6]. Among patients with lung cancer, up-regulation of TGF-β can accelerate cancer cells invasion and metastasis via triggering EMT, therefore, up-regulation of TGF-β has been viewed as an indicator of poor prognosis [7]. TGF-β triggers EMT mainly through SMAD signaling pathway. The activation of TGF-β/SMAD signaling pathway facilitates the phosphorylation of SAMD2 and SMAD3, simultaneously upregulation of p-SMAD2 /p-SMAD3 can activate specific target genes transcription. Downregulation of E-cadherin and upregulation of N-cadherin have a highly connection with phosphorylation of SAMD2 and SMAD3, which be viewed as a typical change in TGF-β induced EMT pathogenesis [8–10]. Previous studies have demonstrated that SULF2 can promote the process of carcinogenesis, and several kinds of cancer display abnormal high-level expression of SULF2 [11]. Meanwhile, SULF2 can promote the phosphorylation of SAMD2 and activate TGF-β signaling pathway in hepatic carcinoma [12].

MicroRNAs are endogenous, non-coding regulatory RNAs (18–25 nucleotides) which implicated in the regulation of a large number of target genes and development and metastatic dissemination of tumor [13]. Mechanistic investigations revealed that miR-527 inhibited TGF-β/SMAD signaling pathway via decreasing the expression of two TGF-β effectors, SMAD4 and TβRII (TGFBR2) in human osteosarcoma cells [14], while the role of miR527 in lung cancer has not been reported.

Here we report a mutual relationship between miR-527 and SULF2 as key regulators of TGF-β/SMAD signaling pathway which illuminated the potential mechanism of miR-527 in NSCLC epithelial-mesenchymal transition and metastatic dissemination, hence provided a new therapeutic target for clinical treatment of NSCLC.

2. Materials and method

2.1. Clinical specimens

A total of 38 pairs of lung tumor biopsies and corresponding adjacent tumor biopsies (5 cm from the edge of the tumor) were obtained from NSCLC patients with surgical at the cardiothoracic surgery department in our hospital. No patients underwent radiotherapy or chemotherapy before

surgery. Tumor biopsies were taken from tumor site with more than 70% cancer cells. All cases were confirmed by pathological examination. Written informed consents were obtained from all the patients before the execution of surgery, and this study was approved by the institutional ethical committee of our hospital. Clinical specimens were immediately placed in a collection tube containing RNA protective solution after surgery and another part was fixed with 4% paraformaldehyde, dehydrated, embedded, sliced (4 μm) and mounted on glass slide for the next procedure.

2.2. Reagents

One normal human bronchial epithelial cell line (BEAS-2B) and five NSCLC cell lines (A549, SPC-A-1, H358, H522 and H226) applied in our study were purchased from the Type Culture Collection of Chinese Academy of Sciences (Shanghai, China). RPMI-1640 cell culture medium was from Sigma Co. (St. Louis, MO). SULF2 primers, miR-527 plasmid and dual luciferase vector were synthesized by Sango Biotech (Shanghai, China). Promega Dual-Luciferase system assay was from Hang Seng Biotechnology Co. Ltd (Beijing, China). Polyclonal SULF2, E-cadherin, N-cadherin, p-Samd3, p-Smad, GAPDH antibody and HRP-labeled secondary antibody were all purchased from Abcam. LipofectamineTM2000 and Trizol lysate were obtained from Invitrogen (Carlsbad, CA); PrimeScript RT assay was from Takara Biomed (Beijing, China); PCR kit was from Tiangen Biotech (Beijing, China); BCA protein assay kit was from Multi Sciences (Hangzhou, China). TGF-β1 using for cell culture was obtained from Cell Signaling Technology. The specific inhibitor of TGF-β1, SB-431542, was obtained from Selleck; phase-contrast microscopy was purchased from Cnrico (Beijing, China); Transwell migration assay was from Milipore (USA).

2.3. Cell culture

Normal human bronchial epithelial cell line (BEAS-2B) and NSCLC cell lines （A549、SPC-A-1、H358、 H522 and H226） were grown in RPMI-1640 medium 5% fetal bovine serum (FBS) and incubated in a CO_2 incubator (95% CO_2, 37℃). Cells were grown to 70 to 80% confluence and digested with 0.25% trypsin for passage. Cells were serum-deprived in 0.1% FBS for at 24 hours before performed each trial in the logarithmic phase.

2.4. Verification of the target combination between miR-527 and SULF2

MiR-527 and SULF2 biological binding site predicted by Targetscan.org and tested by dual luciferase assay. SULF2 wild type and mutant 3'-UTR were amplified by PCR and separately co-transfected with miR-527 plasmid or negative plasmid into NSCLC cells. Transient transfection was carried out with Lipofectamine2000 and reduced serum medium. After transfection for 48 hours, cells were collected and luciferase activities were determined by the dual-luciferase system assay kit. Cells were washed for two times, added cell lysate for 15 min, centrifuged, discarded sediment and then added LARⅡ solution. The relative luciferase activity was measured by normalizing firefly luciferase against Renilla luciferase activity. The data was obtained from at least three independent experiments with three replicates performed in each trial.

2.5. RNA interference and transfection

For the transfection, SULF2 and scramble siRNAs were designed by BLOCK-iT™ RNAi Designer website (NC-siRNA: TCACTACAGACGATAGTAA; SULF2-siRNA1: TCAGACATCCAGATAGTAA; SULF2-siRNA2: CCAGATAGTAACAGGACAT; SULF2-siRNA3: GCCTAAGTTGCCAACGGAT). 8μL siRNA (20 μmol/L) was dissolved in 250 μl FBS free DMEM medium and incubated at room temperature for 5min. Next, siRNA solution was mixed with LipofectamineTM 2000 and incubated at room temperature for 20 min. NSCLC cells were seeded in a 6-well plate at a density of 1 × 105/well before transfection. When cells grown to 60~70% confluence, transfection was performed by using LipofectamineTM 2000 delivering siRNA in reduced serum medium. After 48 hours, the transfected cells were collected for RNA and protein determination or or other analysis. All trails were repeated at least three times.

2.6. Immunohistochemistry

Slides with samples were conventionally dewaxed in xylene and dehydrated in gradient concentration alcohol. Subsequently, slides were subjected to epitope retrieval in protein kinase K solution (0.2mg/ml) for 10min, and then incubated with 3% hydrogen peroxide for 10min at indoor temperature. After washing 3 times with PBS (3 min/wash), non-specific binding sites were blocked by 50μl non-immunologic goat serum for 30min. Then the sections were incubated at 4℃ overnight with rabbit polyclonal anti-SULF2 antibody (1:200 dilution) (negative control with rabbit IgG). HRP-labeled secondary anti-rabbit IgG antibody (1:2000 dilution) was incubated for 30 min, and DAB and hematoxylin counterstained. The percentage of positive cells was analyzed and photographed using CAIMAS automatic analysis system at five different scopes. The experiment was repeated at least 3 times.

2.7. RNA extraction and quantitative real-time PCR analysis

Total RNA was extracted from lung cancer tissues and NSCLC cell lines with Trizol reagent. cDNAs were synthesized from the total RNAs using PrimeScript Reverse Transcription Kits in accordance with the manufacturer's instructions. Primer were designed by Primer5.0 software, and the synthetic sequences were as follows. Primer sequences for miR-527 were CTCAAGCTGTGACTGCAAAGG (forward), AATTCACCAAAGGGAAGCACT (reverse) and sequences for SULF2 were CTGTGGGAAGGCTGGGAAGG (forward), TGAGAGTGCGTGCTTGCTTTC (reverse), and U6 used as the endogenous control. The amplification was performed under the following conditions: 95℃ for 5 min, followed by 35 cycles of denaturation at 95℃ for 40 sec, annealing at 57℃ for 40 sec, and extension at 72℃ for 40 sec. This was followed by a final extension at 72℃ for 10 min.

2.8. Western Blot

Cells were washed with PBS 3 times and lysed in radioimmunoprecipitation (RIPA) buffer containing a protease inhibitor mixture, and protein concentration was measured by BCA protein assay kit. Western blot procedures were carried out by established methods using the following

primary antibodies: SULF2 (1:1000), E-cadherin (1:500), N-cadherin (1:100), p-Samd3 (1:500), p-Smad2 (1:300) and GAPDH (1:2500). The secondary antibody was co-incubated with HRP-conjugated goat anti-rabbit IgG (1:2000) for 120 min at 25℃. Specific proteins were detected using the ECL prime western blotting detection system. The intensities of protein bands were quantified using Quantity One software and the data were normalized to the control values. All experiments were independently repeated three times.

2.9. EdU staining

For EdU staining, cultured NSCLC cells were exposed to EdU for 2hours. Then cells were washed with PBS twice, fixed with 4% paraformaldehyde for 30 min at room temperature. After washing with PBS three times, cells were permeabilized with 0.4% Triton X-100 for 10 min. Cells were washed three times, and then incubated with EdU staining cocktail in dark at room temperature for 30 min. After washing with PBS, cells were counterstained with 1xHoechst 33342 for 30 min. Images were acquired by fluorescence microscope.

2.10. Flow Cytometric Analysis

Cells were collected and washed twice with cold PBS and resuspended in 1 × Binding Buffer, and then stained using BD Annexin V Apoptosis Detection Kit according to the manufacturer's instruction.

2.11. Cell migration

Cell migration was measured by transwell and scratch-wound methods. For the scratch-wound migration assay, NSCLC cells were seeded in a 6-well plate and grown to 80% confluence. The cell monolayer was scratched with a pipette tip along the ruler and washed with PBS for three times. Scratch width was photographed on an inverted microscope. The migration area (%) was analyzed in five randomly chosen fields under scope, area at 0 hour/area at 24 hours ×100% was calculated. Cells invasive ability was also evaluated by transwell invasion assay. In conclusion, NSCLC cells were inoculated into the upper chamber of the 24-well plate, and 10% fetal bovine serum was added to the lower chamber. After incubation for 24 hours, migrated cells were stained with 0.1% crystal violet and counted under a phase-contrast microscope.

2.12. Statistical analysis

All data appeared in our study were calculated by SPSS 21.0 software. Quantifications were independently executed at least 3 times. Comparison within groups was made by repeated measures ANOVA (or paired t test when only 2 groups were compared). P values of less than 0.05 were viewed as significant. Error bars on all graphs are presented as the SEM of the mean unless otherwise indicated.

3. Results

3.1. Expression of miR-527/SULF2 in NSCLC tissues and cell lines

In order to investigate the expression of miR527 and SULF2 in NSCLC, 38 pairs of lung cancer tissues and matched non-cancerous tissues specimens from NSCLS patients were selected for study. Immunohistochemistry revealed the expression of SULF2 in the cytoplasm of lung cancer was significantly higher than that in paracancerous biopsies (Figure 1A). Consistently, the expression level of miR-527 was analyzed by real-time PCR. We found that expression of miR-527 in NSCLC tissues was significantly lower than that in paracancerous lung tissues (Figure 1B). We further evaluated miR-527 expression in normal human bronchial epithelial cell (BEAS-2B) and NSCLC cell lines. Consistent with above results, miR-527 expression level was lower in BEAS-2B cells than that in NSCLC cell lines, including A549, SPC-A-1, H358, H522 and H226 (Figure 1C). Among these differences, the expression of miR-527 in H358 cells changed the most compared with other NSCLC cell lines, therefore, H358 cells were selected for subsequent trails. We also down-regulated SULF2 expression in H358 cells by siRNA interference and determined the transfection efficiency by PCR (Figure 1D). The most effective #3 siRNA, which reduced SULF2 80%, was applied for next experiments.

3.2. MiR-527 selectively regulated SULF2 expression in NSCLC cells

According to the detection of predicted SULF2-related miR target genes on the TargetScan website, it was found that miR-527 directly targeted the 3'-UTR of SULF2(Figure 2A). Luciferase reporter assays demonstrated that miR-527 co-transfection with SULF2 significantly decreased the activity of SULF2 compared with normal control group (Figure 2B). Moreover, western blot results showed that overexpression of miR-527 could apparently decrease the expression of SULF2 protein compared with NC mimic group (Figure 2C). All these data confirmed that miR-527 can directly targeted and adjusted the expression of SULF2 in NSCLC cells.

3.3. Overexpression miR-527 or downregulation SULF2 suppressed the proliferation and apoptosis of NSCLC cells via mediating TGF-β/SMAD signaling pathway

Large quantity of studies has demonstrated that TGF-β/SMAD signaling pathway plays a key role in the evolution of lung cancer. By inference, we deduced that miR-527 and SULF2 could regulate proliferation and apoptosis of NSCLC cells targeting TGF-β/SMAD signaling pathway. To testify our deduction, we performed experiment which overexpression miR-527 or knockdown SULF2 in NSCLC cells and involved TGF-β1 for different groups. EDU staining revealed that overexpression of miR-527 could alleviate NSCLC cells proliferation rate compared with NC mimic group, and this effect could be effectively inhibited by TGF-β1 (Figure 3A). Consistently, down-regulation of SULF2 expression could inhibit the proliferation of NSCLC cells, and this effect could be blocked by TGF-β1 (Figure 3A). Another index, apoptosis, was detect by flow cytometric analysis. Intriguingly, compared with NC groups, overexpression of miR-527 or knockdown of SULF2 could facilitate apoptosis of NSCLC cells and also could be obviously restrained by TGF-β1 (Figure 3B). Collectively, these results indicated that miR-527 and SULF2 could regulate

proliferation and apoptosis of NSCLC cells targeting to TGF-β/SMAD signaling pathway.

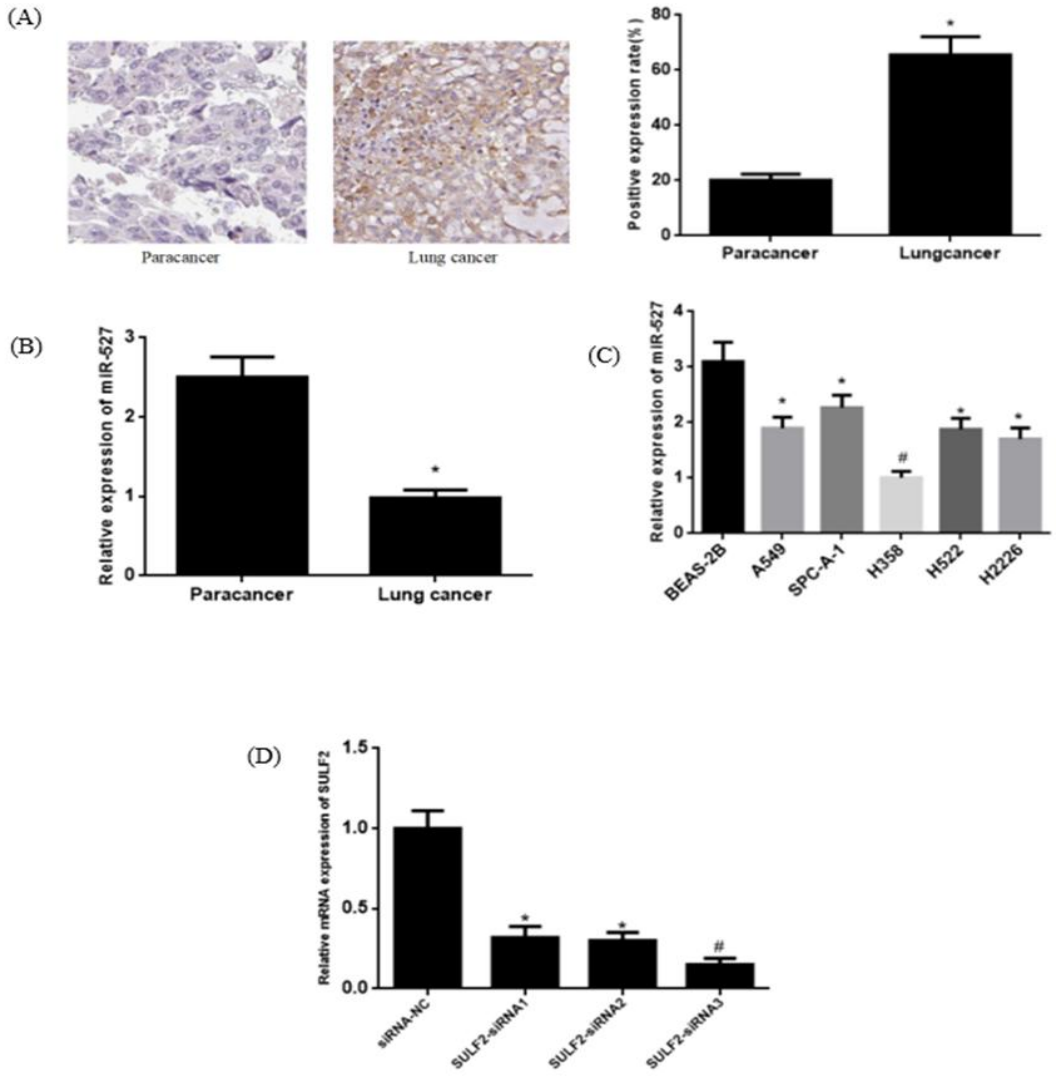

Figure 1. Expression of miR-527/SULF2 in NSCLC tissues and cell lines. (A) SULF2 expression in lung cancer and matched non-cancerous specimens from NSCLS patients was determined by immunohistochemical (IHC) staining. The scale bars indicate 100 μm. Quantitative analysis of SULF2 positive cells in different groups. Bars showed relative value to control (n = 38; *P < 0.05 v.s. paracancer groups). (B) Quantitative real-time RT-PCR analysis of miR-527 expression normalized to GAPDH in NSCLC tissues and matched adjacent tissues (n = 38; *P < 0.05 v.s. paracancer groups). (C) Quantitative real-time RT-PCR analysis of miR-527 expression normalized to GAPDH in normal human bronchial epithelial cell line (BEAS-2B) and five NSCLC cell lines (A549, SPC-A-1, H358, H522 and H226) (n = 10; * P < 0.05 v.s. BEAS-2B cells group; # P < 0.01 v.s. BEAS-2B cells group). (D) Quantitative real-time RT-PCR analysis of down-regulation of SULF2 expression by siRNA (n = 8; *P < 0.05 v.s. NC group; # P < 0.01 v.s. NC group).

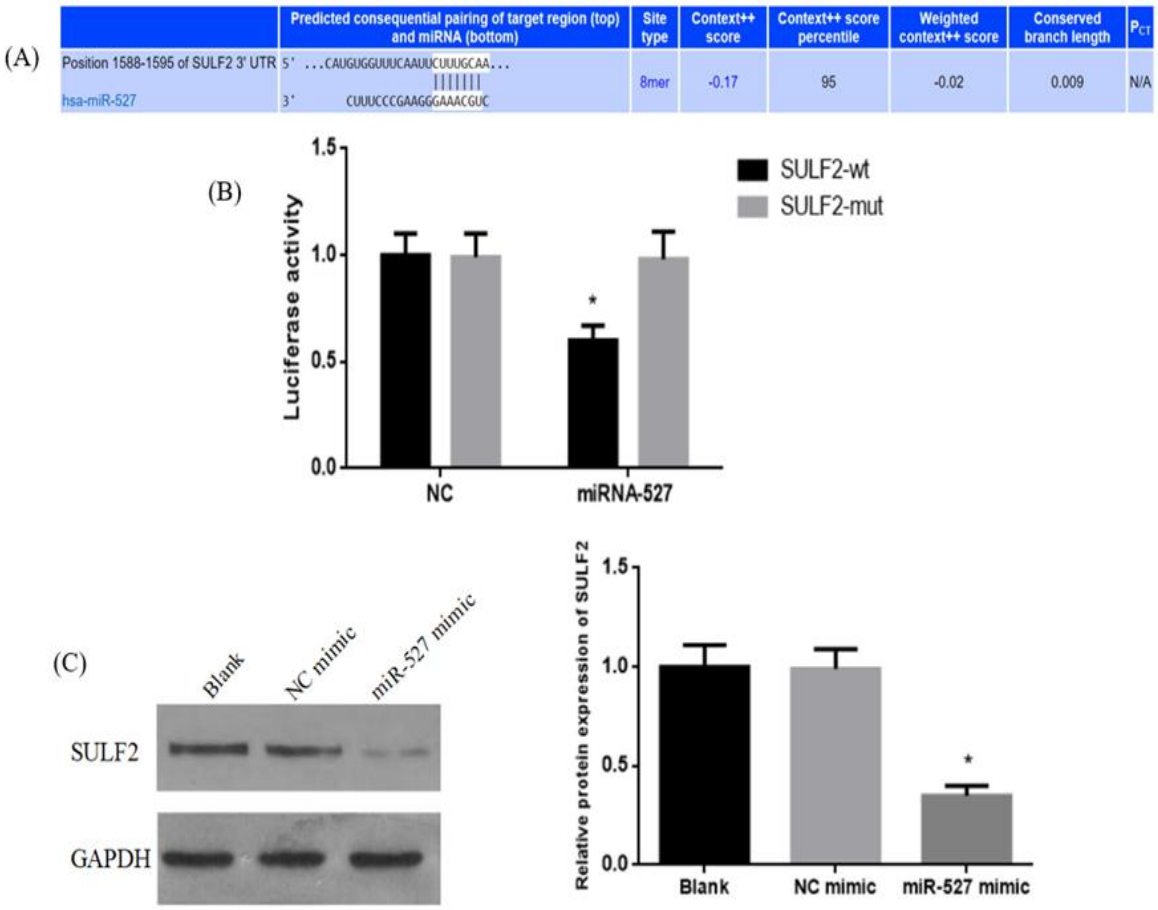

Figure 2. MiR-527 selectively regulated SULF2 expression in NSCLC cells. SULF2 is a target of miR-527. (A) The predicted complementary pairing between target regions of the SULF2 and miR-527 according to Target Scan website. (B) The construct containing the wild-type or mutant SULF2 3'-UTR reporter gene was co-transfected with the miR-527 or negative control (miR-NC) in H358 cells. Two days later, relative renilla luciferase activity was determined and normalized to firefly luciferase activity (n = 8; *P < 0.05 v.s. NC group). (C) Western blot show that overexpression of miR-527 diminished SULF2 expression in H358 cells. GAPDH was used as an internal control. Quantitative analysis of SULF2 expression in different groups. Bars showed relative value to GAPDH. (n = 10; *P < 0.05 v.s. NC group).

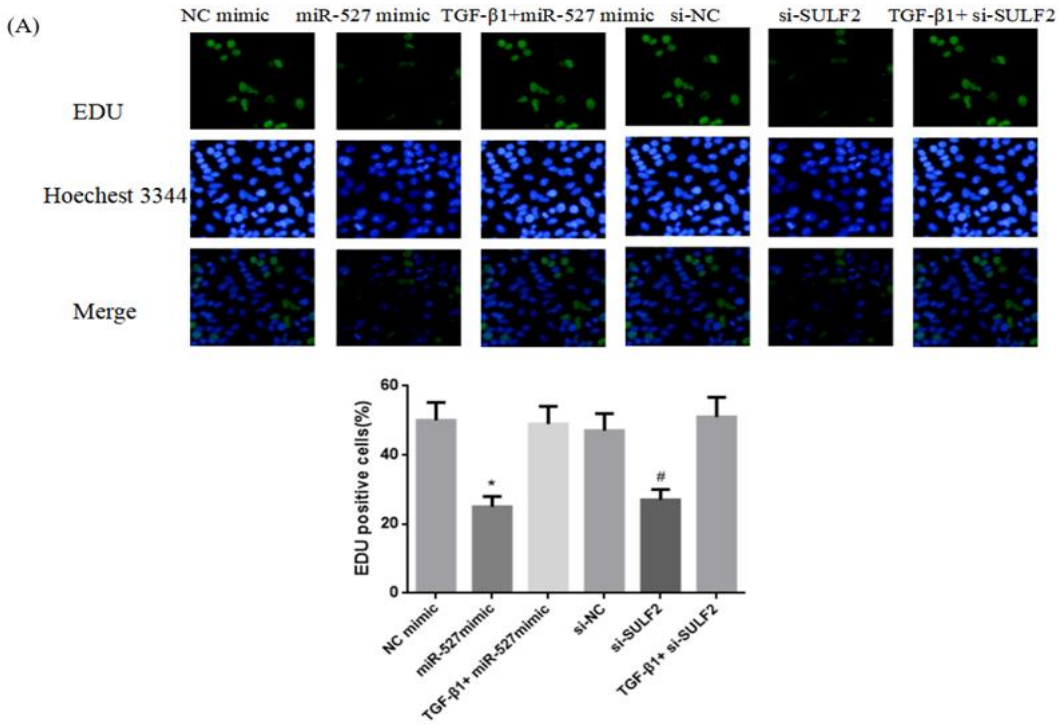
(A)
NC mimic
miR-527 mimic
TGF-β1+miR-527 mimic
si-NC
si-SULF2
TGF-β1+ si-SULF2
EDU
Hoechest 3344
Merge
EDU positive cells(%)
60
40
20
0
*
#
NC mimic
miR-527mimic
TGF-β1+ miR-527mimic
si-NC
si-SULF2
TGF-β1+ si-SULF2

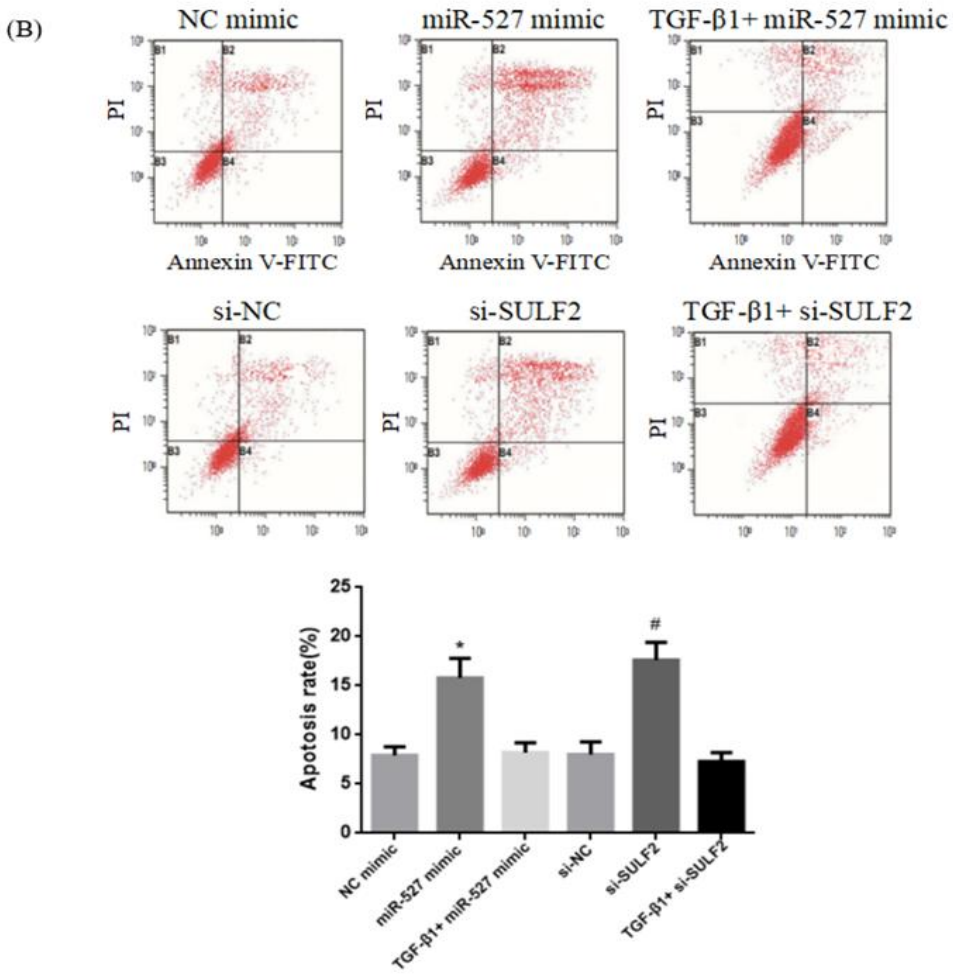
(B)
NC mimic
miR-527 mimic
TGF-β1+ miR-527 mimic
si-NC
si-SULF2
TGF-β1+ si-SULF2
PI
Annexin V-FITC
B1
B2
B3
B4
Apotosis rate(%)
25
20
15
10
5
0
*
#
NC mimic
miR-527 mimic
TGF-β1+ miR-527 mimic
si-NC
si-SULF2
TGF-β1+ si-SULF2

Figure 3. Effect of overexpression miR-527 or downregulation SULF2 on proliferation and apoptosis in NSCLC cells. (A) Effect of miR-527, SULF2 and TGF-β1 on proliferation of H358 cells detected by EDU staining. EDU positive cells is stained green and the nuclei are stained blue. The scale bars indicate 100 μm. The data are presented as the mean ± SEM. (n = 8; *P < 0.05 v.s. NC mimic group；#P < 0.05 v.s. si-NC group). (B) Effect of miR-527, SULF2 and TGF-β1 on apoptosis of H358 cells detected by Annexin V-FITC/PI. The data are presented as the mean ± SEM. (n = 10; *P < 0.05 v.s. NC mimic group；#P < 0.05 v.s. si-NC group).

3.4. Overexpression miR-527 or downregulation SULF2 suppressed the migration of NSCLC cells via mediating TGF-β/SMAD signaling pathway

We have confirmed that miR-527 and SULF2 have a crucial impact on proliferation and apoptosis of NSCLC cells through TGF-β/SMAD signaling pathway. However, invasion and migration are as important as proliferation and apoptosis for the development of tumors [15,16]. On this basis, Transwell and wound-healing assays were used to detect the effects of miR-527 and SULF2 on the migration and invasion of NSCLS cells. The results showed that overexpression of miR-527 or knockdown of SULF2 suppressed migration of NSCLC cells compared with NC group (Figure 4A and 4B). In contrast, when co-incubate with TGF-β1 in indicated groups, migration could be prevented. These results indicated that overexpression of miR-527 or knockdown of SULF2 could inhibit migration and invasion of NSCLS cells, and this effect also could be blocked by TGF-β1.

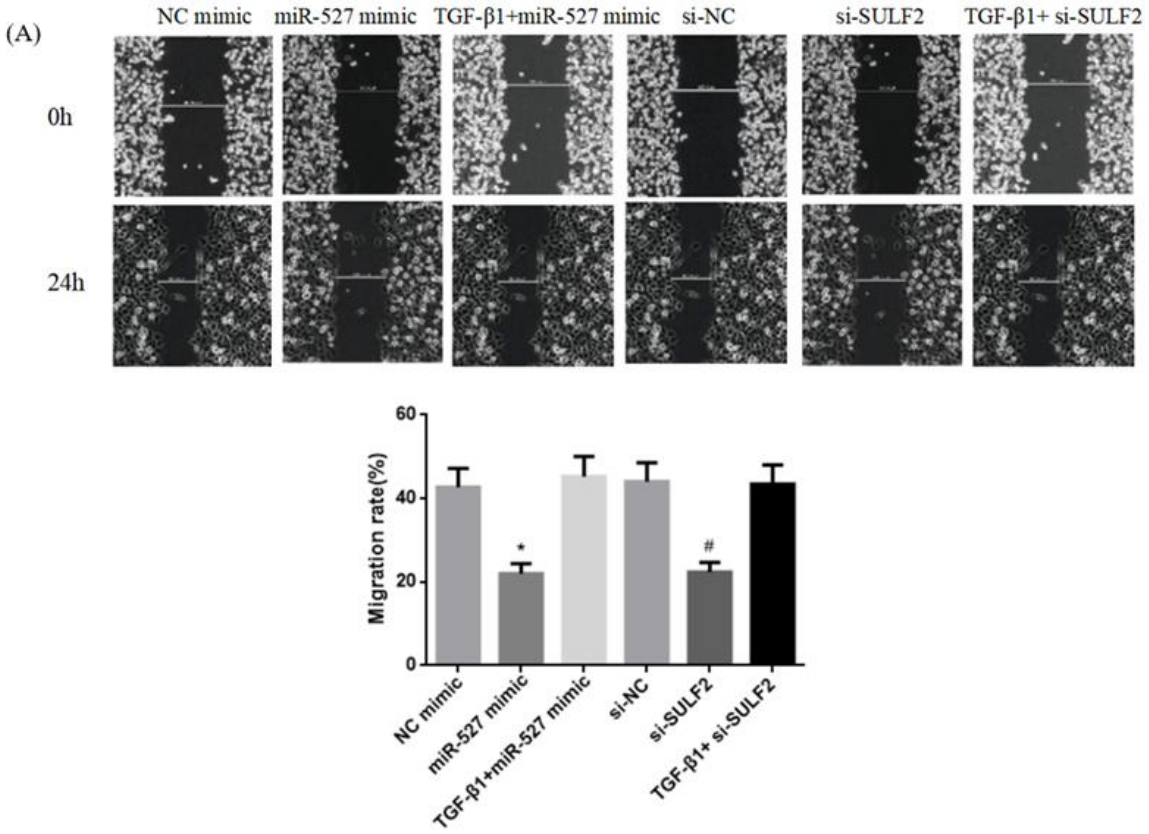

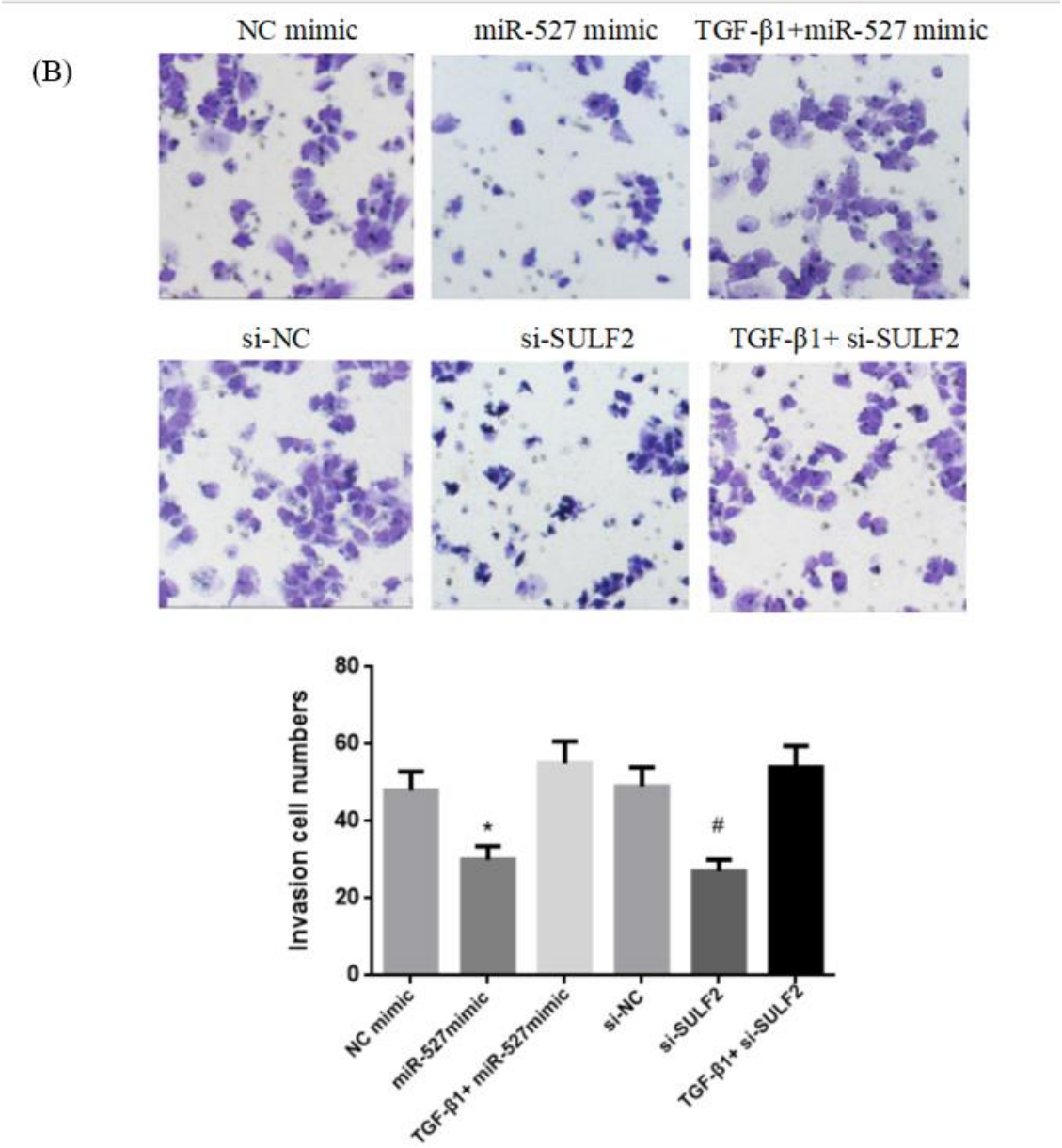

Figure 4. Effect of overexpression miR-527 or downregulation SULF2 on migration in NSCLC cells. (A) Representative images from wound-healing assays using H358 cells at 0 and 24h after scratching show that overexpression miR-527 or downregulation SULF2 inhibits cell migration which blocks by TGF-β1. The wound-healing results are quantified in the histogram. (n = 10; *P < 0.05 v.s. NC mimic group; #P < 0.05 v.s. si-NC group). (B) Representative images from transwell assays using H358 cells at 0 and 24h after scratching show that overexpression miR-527 or downregulation SULF2 inhibits cell migration which blocks by TGF-β1. Cells counts are for the corresponding assays of at least five random microscope fields (migration: ×200 magnification; the scale bars indicate 50 μm). Cell migration and invasion are expressed as a percentage of the control (n = 10; *P < 0.05 v.s. NC mimic group; #P < 0.05 v.s. si-NC group).

3.5. Overexpression miR-527 or downregulation SULF2 inhibited epithelial-mesenchymal transition via mediating TGF-β/SMAD signaling pathway

EMT is regarded as a pivotal step in the invasion and distant metastasis of many tumors. Thus, we hypothesized that overexpressing miR-527 or knocking down SULF2 helps interfere with EMT programs. To investigate our hypothesis, we determined whether the expression levels of EMT markers (E-cadherin, N-cadherin) and TGF-β/SMAD signaling pathway marker (p-Samd3、p-Smad2) changed under conditions of overexpressing miR-527 or knocking down SULF2. As shown by immunoblotting results, overexpression of miR-527 or knockdown of SULF2 led to the up-regulation of E-cadherin, and down-regulation N-cadherin, p-Samd3 and p-Smad2 in NSCLC cells (Figure 5). In contrast, in combination with TGF-β1, these effects were eliminated. Taken together, these data suggested that overexpression of miR-527 or knockdown of SULF2 disturbed NSCLC cells EMT program via suppressing TGF-β/SMAD signaling pathway.

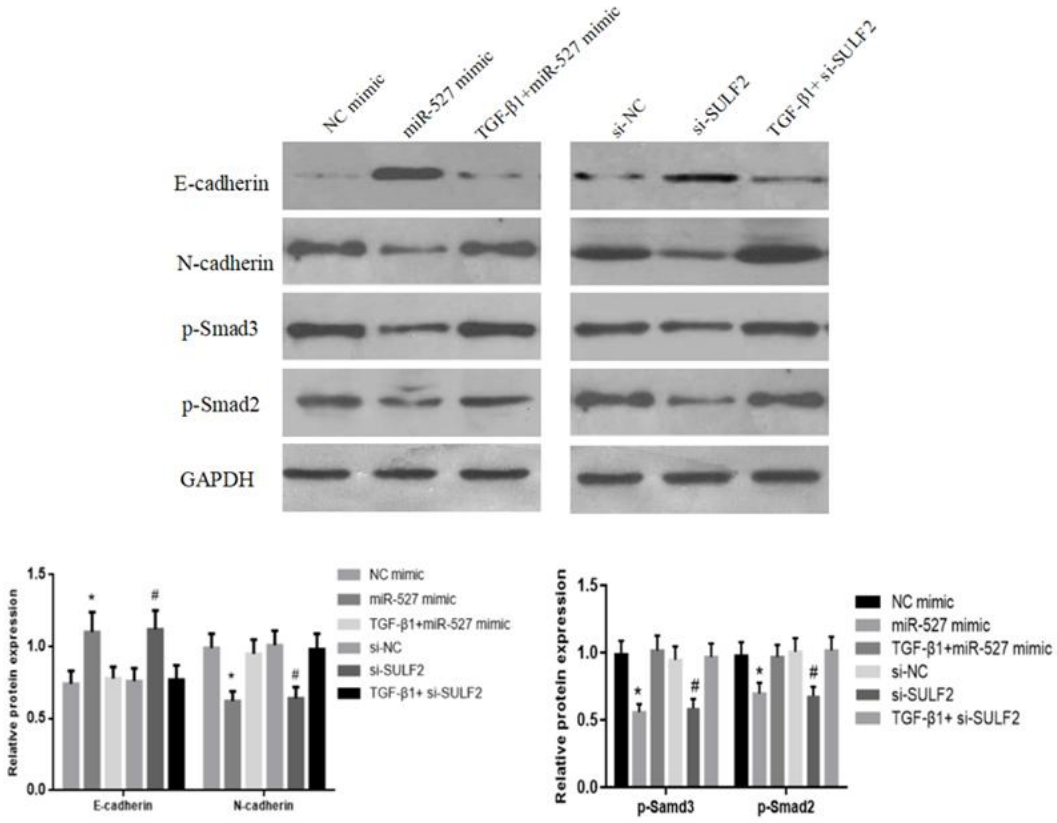

Figure 5. Effect of overexpression miR-527 or downregulation SULF2 on EMT in NSCLC cells. The western blots show that overexpression miR-527 or downregulation SULF2 increases EMT-related markers expression, and decreases TGF-β/SMAD signaling pathway related markers, which reverses by TGF-β1 in H358 cells. GAPDH was used as an internal control. The experiments were performed three times. The protein bands intensity is quantified in the histogram. (n = 8; *P < 0.05 v.s. NC mimic group; #P < 0.05 v.s. si-NC group).

4. Discussion

Lung cancer has been the leading cause of cancer related deaths in China. Up to now, more and more researchers are engaging in prognosis and clinical treatment of lung cancer [17,18]. It has been reported that miRNAs are tightly associated with a variety of carcinomas [19–21]. In our study, we investigated the potential role of miR-527 in NSCLC prognosis. We found that miR-527 evidently down-regulated in lung cancer samples and five NSCLC cell lines (A549, SPC-A-1, H358, H522 and H226), especially in H358 cells. Notably, we also found that expression of SULF2 dramatically upregulated in lung cancer samples compared with corresponding paracancerous biopsies, which means that SULF2 may regulate NSCLC cells proliferation and metastasis. Hence, we forecasted and confirmed the target combination between miR-527 and SULF2 in NSCLC cell lines.

Studies have confirmed that SULF2 promotes the release of growth and angiogenic factors such as FGF-I, FGF-2, VEGF and DSF-I from HS, which can promote the proliferation and metastasis of tumor cells. SULF2 is overexpressed in some lung, breast, brain and liver cancers [22–26]. Studies also reported that SULF2 methylation is a common abnormality in lung cancer cells, suggesting that SULF2 may serve as a prognostic biomarker for better survival in patients with lung cancer [11]. In addition, it is considered that miR-527 can regulate two downstream molecules (p-Samd3、p-Smad2) of TGF-β/SMAD signaling pathway [14]. SULF2 accelerates the phosphorylation of SAMD2 in liver cancer cells [12]. In present study, we found that overexpression of miR-527 or knockdown of SULF2 diminished the activity of TGF-β/SMAD signaling pathway. However, these effects can be able to abolish by TGF-β1 in NSCLC cells.

An increasing number of studies indicate that EMT is a pivotal step which was necessary for epithelial cells to acquire malignant capability [27,28]. TGF-β/SMAD signaling pathway can gear up invasion and metastasis of NSCLC cells, and induce epithelial cells to convert into mesenchymal cells [29,30]. In this study, we confirmed that miR-527 selectively targeted SULF2 and inhibits the process of EMT, which is manifested by the up-regulation of E-cadherin expression in NSCLC cells and the down-regulation of N-cadherin expression. Furthermore, the loss of E-cadherin is viewed as a hallmark of EMT [27,29,31]. The TGF-β/SMAD signaling pathway has been proved to be a major inducer of EMT, thus promoting migration and metastasis of breast cancer [28,32]. We demonstrated for the first time by using Transwell and wound-healing assays that overexpression miR-527 or knockdown SULF2 could suppress the migration of NSCLC cells. When TGF-β1 was involved in our studies, the migration capability of NSCLC cells recovered compared with control group. We also detected the downstream molecules of TGF-β/SMAD signaling pathway and found the expression of p-Smad2 and p-Smad3 was significantly decreased. Taken together, we draw a conclusion that miR-527 targeted SULF2 and down-regulated its expression, concurrently, and inhibits epithelial-mesenchymal transformation and invasion of NSCLC via inhibiting TGF-β/SMAD signaling pathway.

5. Conclusion

In conclusion, we demonstrate for the first time that miR-527 inhibits the EMT and metastasis of NSCLS cells via suppressing the expression of SULF2 and targeting TGF-β/SMAD signaling pathway. miR-527 is expected to be a potential therapeutic target for treating and improving survival rate of patients with NSCLC.

Conflict of interest

The authors declare that they have no conflict of interest.

References

1. J. Su, J. Liao, L. Gao, et al., Analysis of small nucleolar RNAs in sputum for lung cancer diagnosis, *Oncotarget*, **7** (2016), 5131–5142.
2. L. A. Torre, R. L. Siegel and A. Jemal, Lung cancer statistics, *Adv. Exp. Med. Biol.*, **893** (2016), 1–19.
3. L. K. Hou, Y. S. Ma, Y. Han, et al., Association of microRNA-33a molecular signature with non-small cell lung cancer diagnosis and prognosis after chemotherapy, *PLoS One*, **12** (2017), e0170431.
4. B. C. Roy, T. Kohno, R. Iwakawa, et al., Involvement of LKB1 in epithelial-mesenchymal transition (EMT) of human lung cancer cells, *Lung Cancer*, **70** (2010), 136–145.
5. B. Salehi, E. M. Varoni, M. Sharifi-Rad, et al., Epithelial-mesenchymal transition as a target for botanicals in cancer metastasis, *Phytomedicine*, **55** (2019), 125–136.
6. Y. Ke, W. Zhao, J. Xiong, et al., miR-149 inhibits non-small-cell lung cancer cells emt by targeting FOXM1, *Biochem. Res. Int.*, **2013** (2013), 506731.
7. P. Nasarre, R. M. Gemmill, V. A. Potiron, et al., Neuropilin-2 Is upregulated in lung cancer cells during TGF-β1-induced epithelial-mesenchymal transition, *Cancer Res.*, **73** (2013), 7111–7121.
8. L. Wang, X. Tong, Z. Zhou, et al., Circular RNA hsa_circ_0008305 (circPTK2) inhibits TGF-β-induced epithelial-mesenchymal transition and metastasis by controlling TIF1gamma in non-small cell lung cancer, *Mol. Cancer*, **17** (2018), 140.
9. Y. Xiang, Y. Zhang, Y. Tang, et al., MALAT1 modulates TGF-β1-induced endothelial-to-mesenchymal transition through downregulation of miR-145, *Cell Physiol. Biochem.*, **42** (2017), 357–372.
10. L. Fang, S. Wu, X. Zhu, et al., MYEOV functions as an amplified competing endogenous RNA in promoting metastasis by activating TGF-β pathway in NSCLC, *Oncogene*, **38** (2019), 896–912.
11. M. Tessema, C. M. Yingling, C. L. Thomas, et al., SULF2 methylation is prognostic for lung cancer survival and increases sensitivity to topoisomerase-I inhibitors via induction of ISG15, *Oncogene*, **31** (2012), 4107–4116.
12. G. Chen, I. Nakamura, R. Dhanasekaran, et al., Transcriptional induction of periostin by a sulfatase 2-tgf-β1-smad signaling axis mediates tumor angiogenesis in hepatocellular carcinoma, *Cancer Res.*, **77** (2017), 632–645.
13. M. Tantawy, M. G. Elzayat, D. Yehia, et al., Identification of microRNA signature in different pediatric brain tumors, *Genet. Mol. Biol.*, **41** (2018), 27–34.
14. 14. L. Rodriguez Calleja, C. Jacques, F. Lamoureux, et al., ΔNp63α silences a miRNA program to aberrantly initiate a wound-healing program that promotes TGF-β-induced metastasis, *Cancer Res.*, **76** (2016), 3236–3251.
15. A. P. Mishra, B. Salehi, M. Sharifi-Rad, et al., Programmed cell death, from a cancer perspective: An overview, *Mol. Diagn. Ther.*, **22** (2018), 281–295.
16. B. Salehi, P. Zucca, M. Sharifi-Rad, et al., Phytotherapeutics in cancer invasion and metastasis,

Phytother Res., **32** (2018), 1425–1449.
17. C. Lu, H. Wang, S. Chen, et al., Baicalein inhibits cell growth and increases cisplatin sensitivity of A549 and H460 cells via miR-424-3p and targeting PTEN/PI3K/Akt pathway, *J. Cell Mol. Med.*, **22** (2018), 2478–2487.
18. M. Zhang, C. Gao, Y. Yang, et al., MiR-424 Promotes non-small cell lung cancer progression and metastasis through regulating the tumor suppressor gene TNFAIP1, *Cell Physiol. Biochem.*, **42** (2017), 211–221.
19. A. Izzotti, G. A. Calin, P. Arrigo, et al., Downregulation of microRNA expression in the lungs of rats exposed to cigarette smoke, *Faseb J.*, **23** (2009), 806–812.
20. Z. Zhou, X. Niu, C. Li, et al., Inhibition of the growth of non-small cell lung cancer by miRNA-1271, *Am. J. Transl. Res.*, **7** (2015), 1917–1924.
21. X. C. Wang, L. Q. Du, L. L. Tian, et al., Expression and function of miRNA in postoperative radiotherapy sensitive and resistant patients of non-small cell lung cancer, *Lung Cancer*, **72** (2011), 92–99.
22. F. K. Johansson, H. Goransson and B. Westermark, Expression analysis of genes involved in brain tumor progression driven by retroviral insertional mutagenesis in mice, *Oncogene*, **24** (2005), 3896–3905.
23. M. Morimoto-Tomita, K. Uchimura, A. Bistrup, et al., Sulf-2, a proangiogenic heparan sulfate endosulfatase, is upregulated in breast cancer, *Neoplasia*, **7** (2005), 1001–1010.
24. K. Uchimura, M. Morimoto-Tomita, A. Bistrup, et al., HSulf-2, an extracellular endoglucosamine-6-sulfatase, selectively mobilizes heparin-bound growth factors and chemokines: effects on VEGF, FGF-1, and SDF-1, *BMC Biochem.*, **7** (2006), 2.
25. J. P. Lai, D. S. Sandhu, C. Yu, et al., Sulfatase 2 up-regulates glypican 3, promotes fibroblast growth factor signaling, and decreases survival in hepatocellular carcinoma, *Hepatology*, **47** (2008), 1211–1222.
26. H. Lemjabbar-Alaoui, A. van Zante, M. S. Singer, et al., Sulf-2, a heparan sulfate endosulfatase, promotes human lung carcinogenesis, *Oncogene*, **29** (2010), 635–646.
27. J. P. Thiery, H. Acloque, R. Y. Huang, et al., Epithelial-mesenchymal transitions in development and disease, *Cell*, **139** (2009), 871–890.
28. J. Yang and R. A. Weinberg, Epithelial-mesenchymal transition: at the crossroads of development and tumor metastasis, *Dev. Cell*, **14** (2008), 818–829.
29. J. P. Thiery, Epithelial-mesenchymal transitions in tumour progression, *Nat. Rev. Cancer.*, **2** (2002), 442–454.
30. J. Lim and J. P. Thiery, Epithelial-mesenchymal transitions: Insights from development, *Development*, **139** (2012), 3471–3486.
31. D. Hanahan and R. A. Weinberg, Hallmarks of cancer: The next generation, *Cell*, **144** (2011), 646–674.
32. S. Lamouille, J. Xu and R. Derynck, Molecular mechanisms of epithelial-mesenchymal transition, *Nat. Rev. Mol. Cell Biol.*, **15** (2014), 178–196.